frontiers in Chemistry

REVIEW
published: 29 January 2021
doi: 10.3389/fchem.2020.568063

Application of Plasmonic Metal Nanoparticles in TiO_2-SiO_2 Composite as an Efficient Solar-Activated Photocatalyst: A Review Paper

Collin G. Joseph[1,2,3], Yun Hin Taufiq-Yap[4,5,3], Baba Musta[2], Mohd Sani Sarjadi[3] and L. Elilarasi[1,6]*

[1]Sonophotochemistry Research Group, Faculty of Science and Natural Resources, Universiti Malaysia Sabah, Kota Kinabalu, Sabah, [2]Water Research Unit, Faculty of Science and Natural Resources, Universiti Malaysia Sabah, Kota Kinabalu, Sabah, [3]Industrial Chemistry Programme, Faculty of Science and Natural Resources, Universiti Malaysia Sabah, Kota Kinabalu, Sabah, [4]Chancellery Office, Universiti Malaysia Sabah, Kota Kinabalu, Sabah, [5]Catalysis Science and Technology Research Centre, Faculty of Science, Universiti Putra Malaysia, Serdang, Malaysia, [6]Centre of Foundation, Language and Malaysian Studies, International University of Malaya-Wales, Kuala Lumpur, Malaysia

OPEN ACCESS

Edited by:
Sivakumar Ponnusamy, Arignar Anna Government Arts College, India

Reviewed by:
Senthil Subramaniyam, Erode Sengunthar Engineering College, India
Shanmugam Palanisamy, Anna University, India
Geetha Arumugam, Anna University, India

***Correspondence:**
Collin G. Joseph
collin@ums.edu.my

Specialty section:
This article was submitted to Catalysis and Photocatalysis, a section of the journal Frontiers in Chemistry

Received: *31 May 2020*
Accepted: *18 December 2020*
Published: *29 January 2021*

Citation:
Joseph CG, Taufiq-Yap YH, Musta B, Sarjadi MS and Elilarasi L (2021) Application of Plasmonic Metal Nanoparticles in TiO_2-SiO_2 Composite as an Efficient Solar-Activated Photocatalyst: A Review Paper. Front. Chem. 8:568063. doi: 10.3389/fchem.2020.568063

Over the last decade, interest in the utilization of solar energy for photocatalysis treatment processes has taken centre-stage. Researchers had focused on doping TiO_2 with SiO_2 to obtain an efficient degradation rate of various types of target pollutants both under UV and visible-light irradiation. In order to further improve this degradation effect, some researchers resorted to incorporate plasmonic metal nanoparticles such as silver and gold into the combined TiO_2-SiO_2 to fully optimize the TiO_2-SiO_2's potential in the visible-light region. This article focuses on the challenges in utilizing TiO_2 in the visible-light region, the contribution of SiO_2 in enhancing photocatalytic activities of the TiO_2-SiO_2 photocatalyst, and the ability of plasmonic metal nanoparticles (Ag and Au) to edge the TiO_2-SiO_2 photocatalyst toward an efficient solar photocatalyst.

Keywords: TiO_2-SiO_2, plasmonic metal nanoparticles, visible region, photocatalysis, dye

INTRODUCTION

The first breakthrough in producing the photocatalytic effect of TiO_2 was reported by Fujishima-Honda in 1972, in which, photosplitting of water in the presence of TiO_2 was achieved. The team documented the generation of oxygen gas bubbles at the electrode containing TiO_2 placed under an electrical contact with a piece of platinum metal. While both were immersed in water and exposed to light, hydrogen gas was detected at the platinum electrode. The explanation for this effect was that TiO_2, under ultraviolet irradiation with a wavelength lower than 380 nm, produces an electron-hole pairs according to the following equation:

$$TiO_2 + h\nu \rightarrow TiO_2\,(e_{CB^-} + h_{VB^+}) \quad (1)$$

The electron-hole pairs diffuse evenly on the surface of the TiO_2 particle, to react and decompose oxygen and water present in the atmosphere in order to produce $HO^{\bullet}$, hydroxyl radicals, and O_2^-, superoxide ions, according to the following equations:

$$TiO_2\,(h_{VB^+}) + H_2O \rightarrow TiO_2 + H^+ + OH^- \quad (2)$$

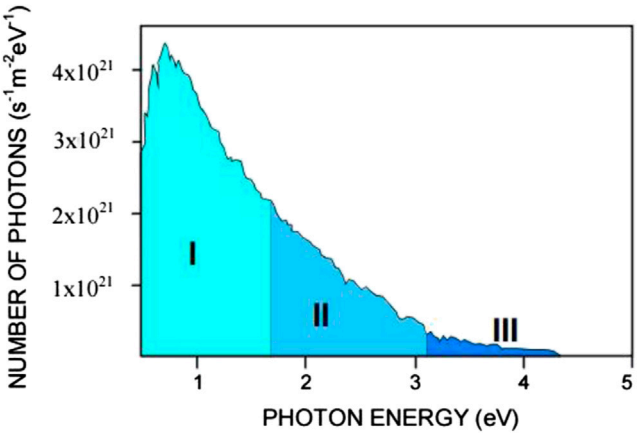

FIGURE 1 | The solar energy spectrum based on the number of photons received per second per unit area of 1 m^2 vs. the photon energy detected on a clear sunny day with the sun at 60° above the horizon. I: IR region, II: visible region, and III: UV region cited by Choi, 2007 which was originally adapted from Oriel-Instruments (Book of Photon Tools, Oriel-Instruments, 1999).

$$TiO_2\,(h_{VB^+}) + OH \rightarrow TiO_2 + OH \quad (3)$$

$$TiO_2\,(e_{CB^-}) + O_2 \rightarrow TiO_2 + O_2^- \quad (4)$$

These oxidants will disintegrate and restructure the pollutants through redox reactions taking place on the surface of catalyst, into H_2O, CO_2, and mineral acids (Zangeneh et al., 2015). The mineral acids are generated due to presence of heteroatoms, i.e., S, N, and Cl in the organic compounds (Gardin et al., 2010). TiO_2, is a commonly used photocatalyst due to its availability, its efficient photoactivity, highest chemical stability, harmless nature, lowest cost, and ability in mineralizing various organic contaminants including dyes, insecticides, aromatics, alkanes, haloalkanes, alcohols, and surfactants (Gardin et al., 2010; Abdullah et al., 2016).

TiO_2-based photocatalysis has long been utilized as one of the methods to remediate wastewater. The main obstruction for the application of TiO_2 under solar energy is its high recombination rate of photoexcited electron-hole pairs and wide band gap which is 3.2 eV (Liu et al., 2013). Due to its wide band gap, it requires photon energy equals or higher than 3.2 eV, in order to induce the photoexcitation of electrons and holes. Unfortunately, majority of photons in visible region have photon energy less than 3.0 eV (based on **Figure 1**). In order to overcome these restrictions, TiO_2 is prepared as a composite catalyst in which the newly added material enables the utilization of TiO_2 in the visible-light region. For instance, doping $CuBiS_2$, a p-type semiconductor (with a band-gap value of 2.19–2.62 eV) onto TiO_2, enabled the direct utilization of TiO_2 photocatalytic activity in the visible-light region (Abdullah & Kuo, 2015).

Another hindrance in utilizing TiO_2 photocatalysis on an industrial scale is the requirement of a large amount of energy to power the UV lamps, resulting in its high operating costs (Chan et al., 2012). In order to overcome these drawbacks, employing sunlight energy to power the photoexcitation of the electrons and holes in the TiO_2 semiconductor would be most ideal. The tapping of solar energy to drive the remediation of wastewater by photocatalysis processes will enable the classification of conventional photocatalysis methods as renewable energy with green technology characteristics.

Due to these benefits, many investigators are currently working on extending the application of TiO_2 photocatalysis into visible-light region. In order to achieve this, one of the methods focused on is the synthesizing of SiO_2-modified TiO_2 photocatalysts which have shown remarkable efficiency under visible-light region.

TIO_2-SIO_2 PHOTOCATALYSIS

Effect of SiO_2 on Specific Surface Area of TiO_2-SiO_2 Composite

SiO_2 is typically used as a catalyst support or dopant dispersed within the TiO_2 lattice (Liga et al., 2013). This doping affects the TiO_2's fundamental properties and thus influences the photocatalytic activities too. The structure modification of TiO_2 by SiO_2 drastically increases the specific surface area of the TiO_2-based photocatalyst. The high surface area of TiO_2-SiO_2 is due to its high porosity. Structures with high porosity have large internal surface area per weight, and it is this property which provides high accessibility and diffusivity in order to allow molecules to penetrate through pores, resulting in higher degradation of pollutants on the catalyst's surface (Jeon et al., 2015).

The morphological improvement by SiO_2 on the TiO_2's surface is evident from the literature. Balachandran et al. (2014) reported that the BET specific surface area increased from 65 $m^2\,g^{-1}$ for TiO_2 to 75 $m^2\,g^{-1}$ for TiO_2-SiO_2 while the mean pore size calculated from BET isotherms was 10 nm for TiO_2 and 15 nm for TiO_2-SiO_2. Bellardita et al. (2010) reported specific surface area of TiO_2-Cabot SiO_2, TiO_2-Axim SiO_2, and TiO_2-Fly Ash SiO_2 as 177, 49, and 29 $m^2\,g^{-1}$, respectively. Fatimah et al. (2015) reported TiO_2-SiO_2 produced by using rice husk ash as the precursor for SiO_2 with a specific surface area of 91.91 m^2/g with a pore volume of 15.18 cc/g compared to that of rice husk ash with a specific surface area of 25.09 m^2g^{-1} and pore volume of 11.60 cc g^{-1}. These results were reportedly higher than that of TiO_2-SiO_2 synthesized by using tetraethyl orthosilicate (TEOS) as the SiO_2 precursor, resulting in catalyst material with a specific surface area of 59.22 m^2/g and

TABLE 1 | BET surface area and crystallite size values of TiO_2-SiO_2 catalysts.

Photocatalyst	BET surface area ($m^2\,g^{-1}$)	Crystallite size (nm)
TiO_2	92	18
SiO_2	289	NA
10% TiO_2-SiO_2	282	9
20% TiO_2-SiO_2	279	10
30% TiO_2-SiO_2	279	10
40% TiO_2-SiO_2	272	11
50% TiO_2-SiO_2	264	12
1% Ag/30% TiO_2-SiO_2	274	10

pore volume of 14.92 cc/g. **Table 1** shows the BET surface area and crystallite size values of TiO_2-SiO_2 photocatalyst reported by Ramamoorthy et al., 2016.

Data in **Table 1** clearly indicate that the high surface area of TiO_2-SiO_2 is attributed to the high surface area of SiO_2 itself. SiO_2 can be synthesized easily via sol gel with a large surface area and pore volume (Ren et al., 2010; Bahadur et al., 2012) and later can be added into TiO_2 sol, generating composite photocatalyst with increased surface area and pore volume. The enhanced surface area of TiO_2-SiO_2 definitely facilitates in achieving higher photocatalytic activity under solar irradiation.

Effect of SiO_2 on Crystalline Size of TiO_2-SiO_2 Composite

Deposition of SiO_2 onto TiO_2 reduces the overall particle size of TiO_2-SiO_2 composite particles. Based on the spectra from the UV-Vis spectrophotometer, Balachandran et al. (2014) reported absorption peak of maximum absorbance of TiO_2 and TiO_2-SiO_2 at 372 and 352 nm, respectively. The blue shift indicates decrease in particle size due to quantum confinement effect. As shown in **Table 1**, Ramamoorthy et al. (2016) reported the reduction in crystallite size of TiO_2-SiO_2 (9–12 nm) compared to TiO_2 (18 nm). In addition, using data from the SEM and TEM analysis, Balachandran et al. (2014) reported that pure TiO_2 showed irregular morphological structure due to the agglomeration of its particles and has an average diameter of 15–20 nm. Meanwhile, TiO_2-SiO_2 showed regular morphology with an average particle size of 7–10 nm. This proves that the SiO_2-modified TiO_2 photocatalyst consists of smaller particles but with larger surface area.

The reduced size of TiO_2-SiO_2 particles reduces the pathway in which the photoinduced electrons and holes are used to migrate to the active sites on the TiO_2 surface. This increases the efficiency of the redox reactions by electrons and holes while reducing the recombination rate of photoinduced electrons and holes, thus making TiO_2-SiO_2 a better photocatalyst as compared to TiO_2.

Effect of SiO_2 on Surface Acidity of TiO_2-SiO_2 Composite

Many previous researchers have reported high surface acidity of TiO_2-SiO_2 composite which aids in enhancing the photo decomposition of pollutant molecules. According to Wei et al. (2014), TiO_2 exhibits Lewis acidity and SiO_2 does not exhibit any acidity while TiO_2-SiO_2 exhibits both Bronsted and Lewis acidity. For TiO_2-SiO_2 with TiO_2 as the main component, the Lewis acid sites are dominant while the Bronsted acid sites are dominant for TiO_2-SiO_2 with SiO_2 as the major component (Fateh et al., 2013). It should be noted that the Ti/Si atomic ratio can be manipulated to control the acidity of the TiO_2-SiO_2. TiO_2-SiO_2 with atomic ratio of four (Ti:Si = 4) exhibits highest Lewis acidity while TiO_2-SiO_2 with atomic ratio of one (Ti:Si = 1) exhibited highest Bronsted acidity (Wei et al., 2014).

The Ti-O-Si bond, a strong acidic bond, in the TiO_2-SiO_2 composite photocatalyst, results in a charge imbalance due to the different coordination numbers of the Ti and Si metal center. To offset the negative imbalanced charges over Ti-O, a great deal of protons is extracted from H_2O molecules generating HO^- groups, which in turn enhances the surface acidity. The decomposition rate of pollutant molecules is enhanced due to higher amount of hydroxyl groups being on the surface of TiO_2-SiO_2, representing a better photocatalytic performance in visible region compared to TiO_2 (Kibombo et al., 2012; Xu et al., 2015).

The increased surface acidity attracts and adsorbs more hydroxyl groups which later act as hole-scavengers and readily oxidize the adsorbed H_2O molecules. These surface hole-scavenger active sites effectively increase the charge separation and reduce the recombination of photoinduced electrons and holes (Kibombo et al., 2012).

Effect of SiO_2 on Band Gap of TiO_2-SiO_2 Composite

One of the main drawbacks of TiO_2 is the fast recombination of photoinduced electrons and holes which decreases the efficiency of its photocatalytic activity. Deposition of SiO_2 onto TiO_2 caused an increase in the band-gap value of the TiO_2-SiO_2 composite, which is due to the quantum-size effect resulting in an increase in the band-gap value and the interface interaction between the oxide phases, either an SiO_2 matrix or SiO_2 support effect. The interface interaction leads to a formation of Ti-O-Si bonds strongly modifying the electronic structure of the Ti atoms (Panayotov and Yates, 2003).

As an example, the band-gap value of TiO_2 and TiO_2-SiO_2 as reported by Balachandran et al. (2014) was 3.3 and 3.54 eV, respectively. Bellardita et al. (2010) documented the band-gap value of pure TiO_2, TiO_2-Cabot SiO_2, and TiO_2/Axim SiO_2 as 3.00, 3.02, and 2.98 eV, respectively. The increased band gap in TiO_2-SiO_2 indicates that the electrons and holes possess stronger reduction (Kibombo et al., 2012) and oxidation abilities and these abilities enhance the photocatalytic activity of the TiO_2-SiO_2 photocatalyst in visible region.

Effect of SiO_2 on Thermal Stability of TiO_2-SiO_2 Composite

Addition of SiO_2 onto TiO_2 increases the overall thermal stability of TiO_2-SiO_2, thus preventing the conversion from anatase TiO_2 into rutile TiO_2 crystalline structure (Kibombo et al., 2012). **Table 2** shows the specific surface and pore volume of CTS-1 (Ti:Si = 1), CTS-4 (Ti:Si = 4), and TiO_2 as a function of the calcination temperature reported by Wei et al. (2014).

When the calcination temperature increased from 500 to 950°C, the specific surface area decreased from 437.4 to 176.3 $m^2 g^{-1}$ for CTS-1 and from 309.5 to 121.2 $m^2 g^{-1}$ for CTS-4. When the calcination temperature was increased from 500 to 950°C, the pore volume of CTS-1 changed from 1.39 to 0.52 ml g^{-1} and the pore volume of CTS-4 changed from 0.55 to 0.30 ml g^{-1}. Meanwhile, for TiO_2, both specific surface area and pore volume were undetectable after calcination at 650°C or higher due to sintering of particles and collapse of interstitial pores. However, both CTS-1 and CTS-4 are less affected by the

TABLE 2 | Specific surface area and pore volume of CTS-1, CTS-4, and TiO_2 in relation to calcination temperature (source: Wei et al. (2014)).

Calcination temperature (°C)	CTS-1		CTS-4		TiO_2	
	Specific surface area (m^2/g)	Pore volume (ml/g)	Specific surface area (m^2/g)	Pore volume (ml/g)	Specific surface area (m^2/g)	Pore volume (ml/g)
500	437	1.39	222	0.50	94	0.33
650	334	0.88	246	0.57	BDL	0.03
800	287	0.75	205	0.57	BDL	BDL[a]
950	176	0.52	121	0.30	BDL	BDL

[a]*BDL = below detection limit.*

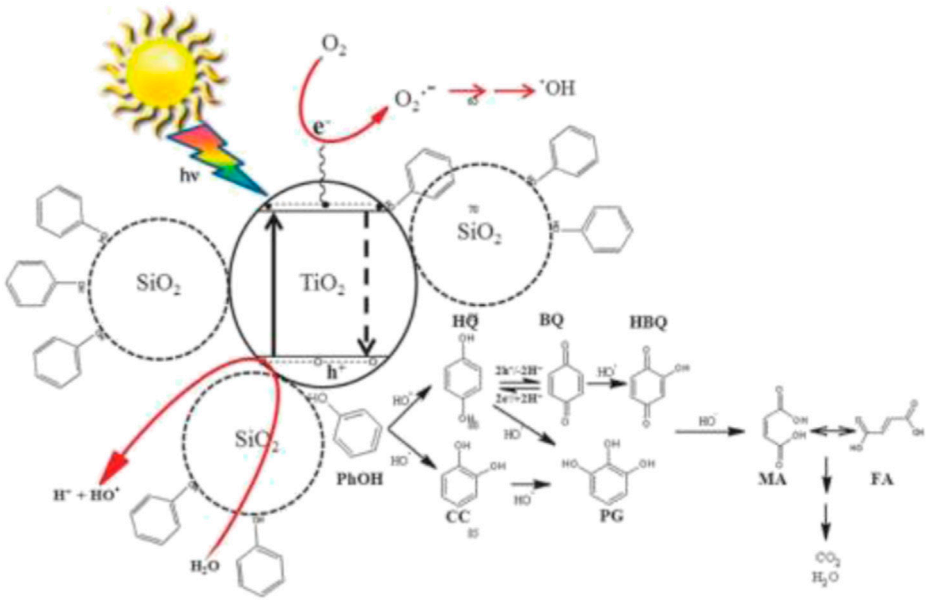

FIGURE 2 | Photocatalytic degradation of phenol over TiO_2-SiO_2 photocatalyst (source: Kibombo et al. (2012)).

increase in calcination temperature due to enhanced thermal stability of TiO_2 with the addition of SiO_2 (Wei et al., 2014).

Photocatalytic Activity of TiO_2-SiO_2 Composite

Binary mixed oxide, TiO_2-SiO_2, has been widely documented as a better photocatalyst compared to TiO_2 alone due to simultaneous roles played by the TiO_2 and SiO_2 as photocatalyst and adsorbent, respectively, according to the reaction mechanism shown in **Figure 2**. The doping of SiO_2 onto TiO_2 enhances the adsorption of pollutant molecules to be near the photoactive center of TiO_2, resulting in more pollutant molecules being broken down, thus producing high degradation rate of pollutant molecules under visible-light region. Due to the presence of more effective adsorption sites in the TiO_2-SiO_2 composite system, the photogenerated holes can reach the sites before recombination with electrons thus further enhancing the photocatalytic activity of TiO_2.

Ramamoorthy et al. (2016) reported that 30% of the TiO_2 incorporated in TiO_2-SiO_2 (200 mg) exhibited 51% degradation of acid orange dye (300 ppm) as compared to only 19% by TiO_2 (200 mg) after 10 h of visible-light irradiation (150 W tungsten filament lamp). Mungondori et al. (2015) reported an absorption band of 366 nm for TiO_2 and 397 nm for TiO_2-SiO_2 analyzed through shift in absorption band edge. This proves that incorporation of SiO_2 into TiO_2 shifts the absorption band of TiO_2 toward the visible-light region.

When the molar ratio of TiO_2 in TiO_2-SiO_2 was increased, the total surface area of TiO_2-SiO_2 decreased causing low photocatalytic activity of the composite catalyst (Ramamoorthy et al., 2016). In a study reported by Jeon et al. (2015), at high molar ratio of TiO_2 (molar ratio of TiO_2 precursor to SiO_2 precursor of 0.05) in the TiO_2-SiO_2, dense thin film with mostly blocked pores was observed. This indicated that at higher concentration of TiO_2 precursor relative to SiO_2 precursor, the size of the pores became smaller if not completely blocked. In contrast, at high SiO_2 precursor molar ratio relative to TiO_2 precursor, the amount of vertically perforated pores increased and formed large micron-sized cracks due to the inability in enduring thermal shrinkage stress as the film thickness increased. Thickness of the film

TABLE 3 | Some of the previous studies on TiO_2-SiO_2 photocatalyst.

Photocatalyst	Synthesis method	Target pollutant	Experimental conditions	Results	References
TiO_2/Cabot-SiO_2, TiO_2/Axim-SiO_2, TiO_2/Fly Ash-SiO_2	Wet method	2-Propanol	Irradiated with UV 500 W medium pressure Hg lamp with 1.3 mW cm^{-2}, 74 μM concentration of 2-propanol	TiO_2-cabot SiO_2 completely mineralized 2-propanol (74 μM concentration) in 6 h. TiO_2/Axim SiO_2 adsorbed half of 2-propanol (initial conc. 30μM) after 6 h. For TiO_2/Fly ash SiO_2 most of the 2-propanol (initial concentration of 30 μM) was adsorbed on the surface	Bellardita et al. (2010)
TiO_2-SiO_2	Sol gel	Acid red 88 (λ_{max} 505 nm)	Experimental conditions: pH 9, 10–40 ppm acid red 88, 4 h sunlight irradiation, 15 min dark adsorption	TiO_2: 96.5% removal % TiO_2-SiO_2: 94.2% removal %	Balachandran et al. (2014)
TiO_2-SiO_2	Sol gel. Rice husk ash as SiO_2 source	Methyl violet (MV)	Experimental conditions: UV-A and UV-B lamps placed 20 cm above the reactor, H_2O_2 as additional oxidant, initial concentration of MV: 1–8ppm	Almost complete degradation of 1 ppm MV in 60 min	Fatimah et al. (2015)
Fibrous nanosilica (KCC-1)-TiO_2, MCM-41/TiO_2> SBA-15/TiO_2	Atomic layer deposition	Methylene blue (1×10^{-5} M). Phenol (1×10^{-5} M)	75 W of UV light 250–385 nm; 25 mg catalyst, 50 ml reaction solution	MB degradation rate: KCC-1/TiO_2> MCM-41/TiO_2> SBA-15/TiO_2, phenol degradation rate: MCM-41/TiO_2 > KCC-1/TiO_2 > SBA-15/TiO_2	Singh et al. (2016)
SiO_2-Fe_2O_3 (5%)-TiO_2-B (5%)-N (5%)	Adsorbed-layer nanoreactor synthesis (ANS)	Methyl orange (MO)	4 W and 40 W fluorescent lamp with rare earth phosphor; 5 h of irradiation	Increase in the amount of Fe/Ti from 1% to 8%, decreased the band-gap energy of SiO_2-TiO_2-Fe_2O_3 from 3.00 to 2.15 eV and decreased the band-gap energy of SiO_2-Fe_2O_3-TiO_2 from 3.00 to 1.89 eV. Increase in the amount of Fe/Ti increased the photocatalytic degradation of MO under 5 h of 40 W room light irradiation	Wang et al. (2016)

has been reported to decrease with increase in molar ratio of SiO_2 in TiO_2/SiO_2 film (Fateh et al., 2013).

When too small amount of SiO_2 (<2%) or too large (>5%) is used to modify TiO_2, it causes lower photocatalytic degradation of TiO_2-SiO_2 as compared to commercial P25 TiO_2. In addition, from the XRD analysis, it was reported that doping a small amount of SiO_2 on TiO_2 will not effectively prevent the rutile phase transformation, which also contributes to a lower photocatalytic activity while a high amount of SiO_2 doping will influence the optical absorption of TiO_2 which is unfavourable in photocatalytic reactions (Kang et al., 2009). **Table 3** presents the gist of the some of the previous studies on TiO_2-SiO_2 photocatalyst.

Challenges in TiO_2-SiO_2 in Solar Photocatalysis

Modification of TiO_2 with SiO_2 alone is insufficient to maximize the utilization of the TiO_2 semiconductor in a solar-energy-powered wastewater remediation process. In order to fully utilize the photocatalytic activity of the TiO_2-SiO_2 in the visible region, there is a need for third material to be added to the TiO_2-SiO_2 in which the third material donates the electrons excited via absorption of photon from sunlight irradiation. Thus, the third material needs to have a low band-gap energy (Eg < 3) in order to utilize the energy directly from the sunlight. Xu et al. (2015) utilized Fe_2O_3, which has a band-gap energy of 2.2 eV, to extend the application of TiO_2 in the visible-light region by coupling with Fe_2O_3.

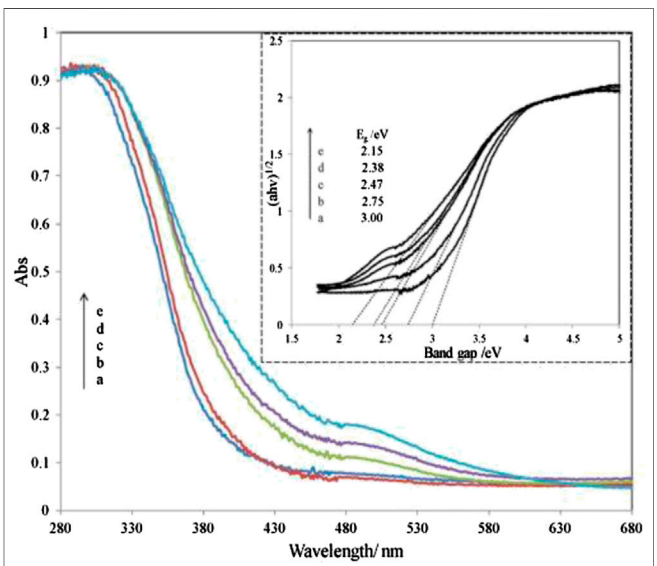

FIGURE 3 | UV-Vis diffuse reflectance spectra of various SiO_2-TiO_2-Fe2O3 combinations. Inset: the plots of (αhv)1/2 vs. photon energy of different catalysts. Ratio percentage of Fe/Ti amount: a, 0%; b, 1%; c, 3%; d, 5%; e, 8% (source: Wang et al. (2016)).

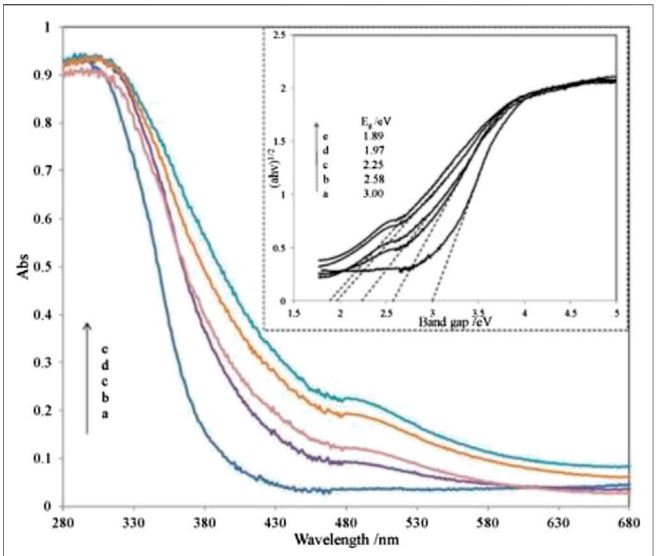

FIGURE 4 | UV-Vis diffuse reflectance spectra of various SiO_2-Fe_2O_3-TiO_2 combinations. Inset: the plots of (αhv)1/2 vs. the photon energy of different catalysts. Ratio percentage of Fe/Ti amount: a, 0%; b, 1%; c, 3%; d, 5%; e, 8% (source: Wang et al. (2016)).

Wang et al. (2016) reported on utilizing Fe_2O_3 coupled TiO_2-SiO_2 photocatalyst irradiated under room light to degrade the methyl orange dye. Based on the diffuse reflectance spectra analysis, the absorption edge of SiO_2-TiO_2 was approximately 400 nm. However, the absorption edge of SiO_2-TiO_2-Fe_2O_3 and SiO_2-Fe_2O_3-TiO_2 is in the visible-light region as shown in **Figures 3**, **4**. This shift directly enables and enhances the photocatalytic activity of TiO_2-based catalyst in the visible-light region due to the narrowing of the band-gap value. Compared to SiO_2-TiO_2-Fe_2O_2, SiO_2-Fe_2O_3-TiO_2 exhibited a higher photocatalytic activity in the visible region due to strong interaction between Fe_2O_3 and TiO_2 and due to the formation of shallow trapping sites for photoinduced electrons and holes.

The codoped SiO_2-Fe_2O_3(5%)-TiO_2 by N and B exhibited high photocatalytic activity of methyl orange under weak room light irradiation (4 W fluorescent lamp with rare earth phosphor) due to synergistic effect of both N doping and Fe_2O_3 coupling which enhanced the visible-light absorbance and reduced the band-gap energy of TiO_2-based catalyst and at the same time, and both N and B doping on TiO_2 caused high separation efficiency for photoinduced electrons and holes (Wang et al., 2016).

DEPOSITION OF PLASMONIC METAL NANOPARTICLES

Another option to maximize the application of TiO_2-SiO_2 photocatalyst in the visible-light region is by incorporating plasmonic metals such as Ag and Au into TiO_2 in order to utilize their ability in absorbing strongly in visible region. Their ability in absorbing of solar photons is attributed to the Localized Surface Plasmon Resonance (LSPR) (Hao et al., 2016). LSPR is defined as collective motions of conduction electrons induced by light irradiation (Chen et al., 2012). Some of the previous attempts to deposit plasmonic metal onto the TiO_2-SiO_2 composite are listed in **Table 4**.

Plasmonic nanoparticles (such as Ag and Au) exhibit a property identified as surface plasmon resonance (SPR) especially in the visible region of the electromagnetic spectrum (Cho and Krishnan, 2013; Abdullah and Kuo, 2015). Many previous research studies deposited Ag/Au nanoparticles onto TiO_2-SiO_2 composite photocatalyst due to their ability to enhance photocatalytic activities by trapping the generated photoelectron and reducing the recombination rate of generated electrons and holes by acting as an electron trap (Chen et al., 2012; Abdullah & Kuo, 2015). The Ag/Au nanoparticles enhance the efficiency of TiO_2-SiO_2 photocatalyst by absorbing the solar photons and transferring the energetic electron, formed via SPR excitation, into the TiO_2 (Hamal and Klabunde, 2010; Linic et al., 2011). This mechanism is demonstrated in **Figure 5**, **6**.

Evidence of higher efficiency achieved by plasmonic metal deposited TiO_2-SiO_2 was reported by Liu et al. (2013). Liu showed that under 4 h of visible irradiation, the TiO_2-SiO_2-Ag photocatalyst exhibited an almost complete degradation of rhodamine B (10ppm) as compared to 80% by TiO_2-Ag and only 30% by neat TiO_2. In comparison, Hayashido et al. (2016) documented that Ag@AgBr/mp-TiO_2 is an efficient photocatalyst in the visible-light region (λ > 400 nm) due to the visible-light activity of Ag@AgBr.

Addition of Ag into TiO_2 modifies the lattice parameters of TiO_2 by generating oxygen vacancies which act as active sites for photocatalysis process, reduces recombination rates of photoexcited electrons and holes due to the formation of Schottky barrier between Ag and TiO_2, reduces band-gap value, and generates defect site Ti^{3+} (Gupta et al., 2006; Chen et al., 2007; Hamal and Klabunde, 2010). Hamal and Klabunde (2010) documented that 5% AgCl-SiO_2, 5% AgBr-SiO_2, and 5% AgI-SiO_2 exhibited band-gap absorption in visible region as shown in **Figure 7** and were able to degrade rhodamine B dye (concentration of 2×10^{-5} M) in the liquid phase and acetaldehyde in the gas phase under visible region (λ > 420 nm). Among these three, the 5% AgI-SiO_2 was found to be the best photocatalyst due to its low band gap and high surface area as well as high stability.

When molar ratio of TiO_2 in the TiO_2-SiO_2 photocatalyst structure is increased, the total surface area of TiO_2-SiO_2 decreases causing low photocatalytic activity of the composite catalyst (Ramamoorthy et al., 2016). In a study reported by Jeon et al. (2015), at high molar ratio of TiO_2 (molar ratio of TiO_2 precursor to SiO_2 precursor of 0.05) in the TiO_2-SiO_2 photocatalyst, a dense thin film with mostly blocked pores was observed. This indicates that at higher concentration of the TiO_2 precursor relative to the SiO_2 precursor, the size of the pores becomes smaller and may be completely blocked. In contrast at high SiO_2 precursor molar ratio relative to TiO_2 precursor, the amount of vertically perforated pores increases and forms large micron-sized cracks due to the inability in enduring thermal shrinkage stress due to the high film thickness. Thickness of the

TABLE 4 | Some of the previous studies on plasmonic metal deposited TiO_2-SiO_2.

Photocatalyst	Synthesis method	Target pollutant	Result	Experimental conditions	References
AgX-SiO_2 (X-Cl, Br, or I)		Acetaldehyde (gas phase). Rhodamine B dye (5.4×10^{-5} M; liquid phase)	Gas phase: under visible irradiation, photoactivity follows the order AgI-SiO_2> AgBr-SiO_2 > AgCl-SiO_2. under UV irradiation, AgI-SiO_2 and AgBr-SiO_2 exhibited similar and higher photocatalytic activity compared to AgCl-SiO_2. Liquid phase: under visible irradiation, only AgI-SiO_2 is able to degrade the rhodamine B dye. Under UV irradiation, photocatalytic activity follows the order AgI-SiO_2> AgBr-SiO_2 > AgCl-SiO_2	UV irradiation (320–400 nm). Visible-light irradiation (420 nm); 0.1 g photocatalyst, total volume 150 ml	Hamal and Klabunde (2010)
TiO_2-SiO_2-Ag	Biomimetic using lysozyme and sol gel	Rhodamine B (10 ppm)	96.9% of RhB degraded by 0.11%Ag/TiO_2-SiO_2, 67.5% by 0.08%Ag/TiO_2-SiO_2, and 31% by 0.04% Ag/TiO_2-SiO_2 under 4 h visible irradiation (λ > 420 nm). Adsorption experiment: 30% RhB adsorbed by TiO_2-SiO_2-Ag compared by only 10% for both TiO_2-Ag and TiO_2	50 mg of catalyst; 50 ml of 10 ppm RhB, 150 W Xenon arc lamp with cutoff filter (λ > 420 nm)	Liu et al. (2013)
Au@SiO_2-TiO_2	Sol gel	Methylene blue (2.4×10^{-5} M)	After 5 h of irradiation with UV_{365nm} and visible light, TiO_2 and SiO_2-TiO_2 degraded about 44% of MB, Au/TiO_2 degraded about 80% MB and Au@SiO_2-TiO_2 degraded about 95%	$UV_{365nm.}$ visible irradiation (400–700 nm) -UV_{365nm}, Xenon lamp with filter (400 nm <λ < 700 nm); 150 klux	Chen et al. (2012)
SiO_2/TiO_2/20%$CuBiS_2$/2%Ag	Sol gel Ag deposited via photoinduction. $CuBiS_2$ deposited via precipitation	Acid black 1 (10ppm)	Under UV irradiation: 100% degradation of AB1 in 5 min. Under visible-light irradiation: 100% degradation of AB1 in 30 min	Visible irradiation with 150 W incandescent halogen lamp and ultraviolet irradiation with 450 W xenon light with cutoff filter (λ > 400 nm)	Abdullah and Kuo (2015)
Ag25/SiO_2/TiO_2	Modified Stober process; Au/SiO_2 and Ag/SiO_2 deposited onto TiO_2 by using maleic acid	1.50×10^{-4} M aqueous salicylic acid (SA) and 1.50×10^{-4} M aniline (A)	Under UV-visible-light irradiation. SA: 3.8 times higher than bare TiO_2. A: 2.5 times higher than bare TiO_2	UV-visible: 300 W Xe lamp with water filter to cutoff IR.	Lee et al. (2017a)
SiO_2-Ag@ TiO_2	Sol gel; impregnation	10 mg/L of TC 2×10^{-5} M of RhB, MB, and MV	60% degradation of TC; 95.9% RhB dye	120 min; visible irradiation, 350 W with UV cut filter (λ > 420 nm)	Zhang et al. (2018)
M-TiO_2/SiO_2 (M: Pt^{4+}, Pd^{2+}, and Ag^{+})	Photodeposition method using 8 W blacklight lamp (365 nm) for 15 h in N_2 atmosphere	Brilliant red K-2G (K-2G) and cationic blue X-GRL (CBX)	300 W high pressure mercury lamp (330–550 nm)	Pt-modified catalyst demonstrated a 2.8 times higher photoactivity than the TiO_2/SiO_2 for the photodegradation of K-2G. However, this catalyst had a lower degradation rate for CBX.	Hu et al. (2003)
TiO_2-SiO_2 (TS1) materials doped with Ag and Pt nanoparticles	TiO_2-SiO_2 was prepared by the sol-gel method. Ag- and Pt-based photocatalysts were prepared by photodeposition (400 W medium pressure mercury lamp)	Phenol	Solar simulator box equipped with a Xe lamp (450 W m^{-2}) emitting the solar spectrum	TS1-Ag-1.0 and TS1-Pt-1.0, respectively, showed an increase in the photocatalytic activity up to two and five times higher than TS1	Matos et al. (2018)

(Continued on following page)

TABLE 4 | (*Continued*) Some of the previous studies on plasmonic metal deposited TiO_2-SiO_2.

Photocatalyst	Synthesis method	Target pollutant	Result	Experimental conditions	References
Core/shell nanostructures SiO_2/TiO_2 doped with Au nanoparticles	A combination of methods to prepared each component	Methyl orange (MO)	The UV light (I < 400 nm) filtered using a UV shield flim (SK-2, Sunnano) to produce only visible light at a power density of 80 ± 2.5 mW cm^{-2}	The photocatalyst decomposed 1% of MO solution in 15 ml deionized water in 1 h under the visible light	Lee at al. (2017b)
Ag-coated SiO_2@TiO_2 (Ag-SiO_2@TiO_2) core-shell nanocomposites	Hydrothermal process and photodeposition (high-pressure Hg UV lamp for 60 min)	Phenol and methylene blue	500 W high-pressure mercury lamp	Ag nanoparticles improved the photocatalytic activity of SiO_2@TiO_2 core-shell nanoparticle improved the degradation of phenol and methylene blue	Fu et al. (2019)

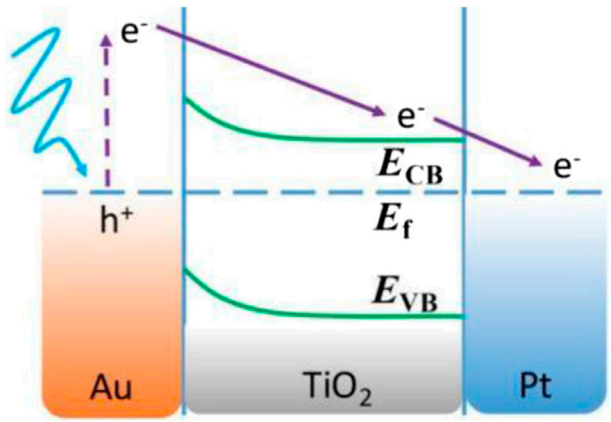

FIGURE 5 | Schematic representations of excited electron generated in AuNS and transfer to the TiO_2 CB, where ECB, Ef, and EVB represent the energies of the conduction band, Fermi level, and valence band, respectively (source: Shi et al. (2016)).

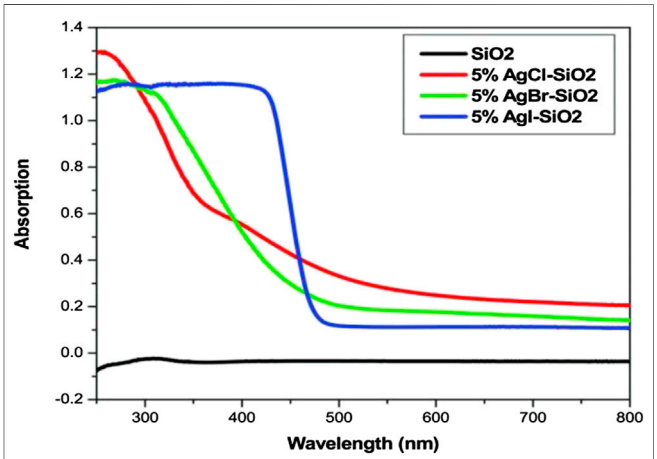

FIGURE 7 | UV-Vis spectrophotometer absorption spectra of 5% silver halide supported on silica (Hamal and Klabunde (2010)).

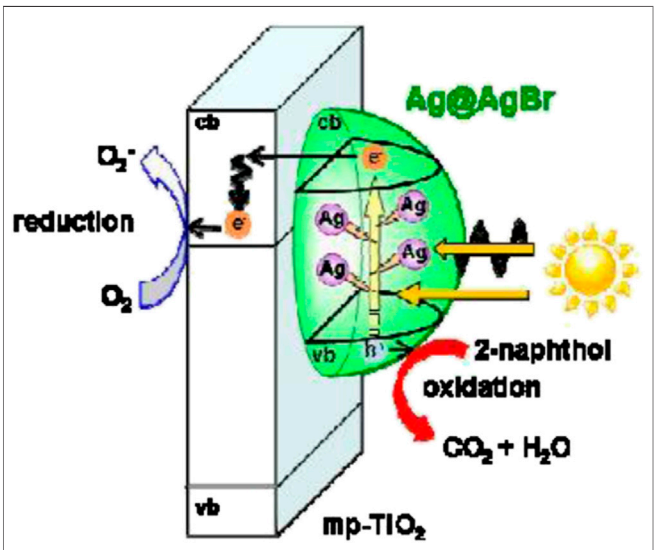

FIGURE 6 | Reaction mechanism of the Ag@AgBr/mp-TiO_2 photocatalyst under visible-light irradiation (source: Hayashido et al., 2016).

film has been reported to decrease with the increase in molar ratio of SiO_2 in TiO_2/SiO_2 film (Fateh et al., 2013).

When the amount of SiO_2 used to modify the TiO_2 is too small (<2%) or too large (>5%), it causes lower photocatalytic degradation of TiO_2-SiO_2 as compared to commercial P25 TiO_2. In addition, from the XRD analysis, it was reported that doping small amount of SiO_2 on TiO_2 will not effectively prevent rutile phase transformation, which also produces lower photocatalytic activity while high mount of SiO_2 doping will influence the optical absorption of TiO_2 which is not favourable in photocatalytic reactions (Kang et al., 2009).

Lee et al. (2017a) employed the citrate reduction method to prepare Au and polyol method to prepare Ag nanoparticles, respectively. After that, modified Stober process was employed to coat Au and Ag surfaces with SiO_2. The prepared composites were later deposited onto TiO_2 (Degussa P25) by employing maleic acid as an anchoring agent. Lee et al. (2017b) reported that Ag@SiO_2-doped TiO_2 nanoparticles are significantly more effective in photocatalytic activity than Ag-doped TiO_2. Ag25@SiO_2/TiO_2 exhibited the highest activity in decomposing aqueous salicylic acid and aniline under UV-visible light irradiation; which was 3.8 and 2.5 times,

respectively, that of the bare TiO_2. The authors attributed the high photocatalytic efficiency of Ag25@SiO_2/TiO_2 to strong LSPR effect of Ag.

Zhang et al. (2018) found that SiO_2-Ag/TiO_2 (SAT) showed enhanced visible-light activity and UV light activity compared to SiO_2-TiO_2/Ag (STA) for degrading tetracycline and traditional dyes. According to them, SiO_2 serves as an efficient support for the Ag nanoparticle immobilization; meanwhile, TiO_2 retains the hierarchical structure and prevents agglomeration of Ag nanoparticles during photocatalytic reaction. They attributed the excellent photocatalytic activity of SAT to improve the transport path of photogenerated electrons, diminished recombination probability of electron-hole pairs, and reduced threat of oxidation and corrosion. It should be noted that the SAT retained its photocatalytic efficiency even after five consecutive runs.

CONCLUSION

Plasmonic metal particle-incorporated TiO_2-SiO_2 composite plays an essential role as a solar photocatalyst which can transform solar energy into chemical energy for application in photocatalysis. Various methods and strategies were presented in this work that highlighted this incorporation, yielding different results. By taking advantage of three synergistic effects that can influence the photocatalytic activity of TiO_2, ability to absorb solar photons by plasmonic metal nanoparticles (Ag or Au), and high adsorption activity by SiO_2, it is possible to utilize the renewable solar energy for water and wastewater remediation effectively. With greater focus on this composite photocatalyst, the next few years will bring major advancement in utilizing the Ag/Au-incorporated TiO_2-SiO_2 in water and wastewater treatment plants at an industrial scale.

AUTHOR CONTRIBUTIONS

CJ supervised the student, visualised, wrote, and edited the manuscript. YH wrote and edited the manuscript. BM made funding acquisition and edited the manuscript. MS made funding acquisition and edited the manuscript. LE conducted the research and investigation process and wrote the original draft.

FUNDING

This research was supported by the Research and Innovation Management Center of University Malaysia Sabah (grant no. SBK0354-2017), and it is gratefully acknowledged.

REFERENCES

Abdullah, H., Kuo, D. H., Lee, J. Y., and Wu, C. M. (2016). Recyclability of thin nylon film-supported p-$CuBiS_2$/n-TiO_2 heterojunction-based nanocomposites for visible light photocatalytic degradation of organic dye. *Appl. Phys. A*. 122 (8), 750. doi:10.1007/s00339-016-0276-4

Abdullah, H., and Kuo, D. H. (2015). Photocatalytic performance of Ag and $CuBiS_2$ nanoparticle-coated SiO_2@ TiO_2 composite sphere under visible and ultraviolet light irradiation for azo dye degradation with the assistance of numerous nano p–n diodes. *J. Phys. Chem. C*. 119 (24), 13632–13641. doi:10.1021/acs.jpcc.5b01970

Bahadur, J., Sen, D., Mazumder, S., Sastry, P. U., Paul, B., Bhatt, H., et al. (2012). One-step fabrication of thermally stable TiO_2/SiO_2 nanocomposite microspheres by evaporation-induced self-assembly. *Langmuir* 28 (31), 11343–11353. doi:10.1021/la3022886

Balachandran, K., Venckatesh, R., Sivaraj, R., and Rajiv, P. (2014). TiO_2 nanoparticles versus TiO_2–SiO_2 nanocomposites: a comparative study of photo catalysis on acid red 88. *Spectrochim. Acta Mol. Biomol. Spectrosc.* 128, 468–474. doi:10.1016/j.saa.2014.02.127

Bellardita, M., Addamo, M., Di Paola, A., Marcì, G., Palmisano, L., Cassar, L., et al. (2010). Photocatalytic activity of TiO_2/SiO_2 systems. *J. Hazard Mater*. 174 (1–3), 707–713. doi:10.1016/j.jhazmat.2009.09.108

Chan, P. Y., El-Din, M. G., and Bolton, J. R. (2012). A solar-driven UV/Chlorine advanced oxidation process. *Water Res*. 46 (17), 5672–5682. doi:10.1016/j.watres.2012.07.047

Chen, H. W., Ku, Y., and Kuo, Y. L. (2007). Photodegradation of o-cresol with Ag deposited on TiO_2 under visible and UV light irradiation. *Chem. Eng. Technol.* 30 (9), 1242–1247. doi:10.1002/ceat.200700196

Chen, J. J., Wu, J. C., Wu, P. C., and Tsai, D. P. (2012). Improved photocatalytic activity of shell-isolated plasmonic photocatalyst Au@ SiO_2/TiO_2 by promoted LSPR. *J. Phys. Chem. C*. 116 (50), 26535–26542. doi:10.1021/jp309901y

S. H. Cho and S. Krishnan (Editiors) (2013). *Cancer nanotechnology: principles and applications in radiation oncology*. (Boca Raton, FL: CRC Press), 296.

Choi, K. S. (2007). *Band gap tuning of zinc oxide films for solar energy conversionA CASPiE Module*. West Lafayette, Ind: Purdue University, 38.

Fateh, R., Dillert, R., and Bahnemann, D. (2013). Preparation and characterization of transparent hydrophilic photocatalytic TiO_2/SiO_2 thin films on polycarbonate. *Langmuir* 29 (11), 3730–3739. doi:10.1021/la400191x

Fatimah, I., Said, A., and Hasanah, U. A. (2015). Preparation of TiO_2-SiO_2 using rice husk ash as silica source and the kinetics study as photocatalyst in methyl violet decolorization. *Bull. Chem. React. Eng. Catal.* 10 (1), 43–49. doi:10.9767/bcrec.10.1.7218.43-49

Fu, N., Ren, X.-C., and Wan, J.-X. (2019). Preparation of Ag-coated SiO_2@TiO_2 core-shell nanocomposites and their photocatalytic applications towards phenol and methylene blue degradation. *J. Nanomater*. 2019, 8. doi:10.1155/2019/8175803

Gardin, S., Signorini, R., Pistore, A., Giustina, G. D., Brusatin, G., Guglielmi, M., et al. (2010). Photocatalytic performance of hybrid SiO_2–TiO_2 films. *J. Phys. Chem. C*. 114 (17), 7646–7652. doi:10.1021/jp911495h

Gupta, A. K., Pal, A., and Sahoo, C. (2006). Photocatalytic degradation of a mixture of Crystal Violet (Basic Violet 3) and Methyl Red dye in aqueous suspensions using Ag^+ doped TiO_2. *Dyes Pigments* 69 (3), 224–232. doi:10.1016/j.dyepig.2005.04.001

Hamal, D. B., and Klabunde, K. J. (2010). "Heterogeneous photocatalysis over high-surface-area silica-supported silver halide photocatalysts for environmental remediation,"in *Nanoscale materials in chemistry: environmental applications*. (Washington: American Chemical Society), 191–205.

Hao, C. H., Guo, X. N., Pan, Y. T., Chen, S., Jiao, Z. F., Yang, H., et al. (2016). Visible-light-driven selective photocatalytic hydrogenation of cinnamaldehyde over Au/SiC catalysts. *J. Am. Chem. Soc*. 138 (30), 9361–9364. doi:10.1021/jacs.6b04175

Hayashido, Y., Naya, S. I., and Tada, H. (2016). Local electric field-enhanced plasmonic photocatalyst: formation of Ag cluster-incorporated AgBr nanoparticles on TiO_2. *J. Phys. Chem. C*. 120 (35), 19663–19669. doi:10.1021/acs.jpcc.6b04894

Hu, C., Tang, Y., Jiang, Z., Hao, Z., Tang, H., and Wong, P. K. (2003). Characterization and photocatalytic activity of noble-metal-supported surface TiO_2/SiO_2. *Appl. Catal. Gen.* 253 (2), 389–396. doi:10.1016/S0926-860X(03)00545-3

Jeon, H., Lee, C. S., Patel, R., and Kim, J. H. (2015). Well-organized meso-macroporous TiO_2/SiO_2 film derived from amphiphilic rubbery comb

copolymer. *ACS Appl. Mater. Interfaces*. 7 (14), 7767–7775. doi:10.1021/acsami.5b01010

Kang, C., Jing, L., Guo, T., Cui, H., Zhou, J., and Fu, H. (2009). Mesoporous SiO_2-modified nanocrystalline TiO_2 with high anatase thermal stability and large surface area as efficient photocatalyst. *J. Phys. Chem. C*. 113 (3), 1006–1013. doi:10.1021/jp807552u

Kibombo, H. S., Peng, R., Rasalingam, S., and Koodali, R. T. (2012). Versatility of heterogeneous photocatalysis: synthetic methodologies epitomizing the role of silica support in TiO_2 based mixed oxides. *Catal. Sci. Technol*. 2 (9), 1737–1766. doi:10.1039/C2CY20247F

Lee, J. E., Bera, S., Choi, Y. S., and Lee, W. I. (2017a). Size-dependent plasmonic effects of M and M@ SiO_2 (M= Au or Ag) deposited on TiO_2 in photocatalytic oxidation reactions. *Appl. Catal. B Environ*. 214, 15–22. doi:10.1016/j.apcatb.2017.05.025

Lee, R., Kumaresan, Y., Yoon, S. Y., Um, S. H., Kwon, I. K., and Jung, G. Y. (2017b). Design of gold nanoparticles-decorated SiO_2@TiO_2 core/shell nanostructures for visible light-activated photocatalysis. *RSC Adv*. 7 (13), 7469–7475. doi:10.1039/C6RA27591E

Liga, M. V., Maguire-Boyle, S. J., Jafry, H. R., Barron, A. R., and Li, Q. (2013). Silica decorated TiO_2 for virus inactivation in drinking water–simple synthesis method and mechanisms of enhanced inactivation kinetics. *Environ. Sci. Technol*. 47 (12), 6463–6470. doi:10.1021/es400196p

Linic, S., Christopher, P., and Ingram, D. B. (2011). Plasmonic-metal nanostructures for efficient conversion of solar to chemical energy. *Nat. Mater*. 10 (12), 911–921. doi:10.1038/nmat3151

Liu, C., Yang, D., Jiao, Y., Tian, Y., Wang, Y., and Jiang, Z. (2013). Biomimetic synthesis of TiO_2–SiO_2–Ag nanocomposites with enhanced visible-light photocatalytic activity. *ACS Appl. Mater. Interfaces* 5 (9), 3824–3832. doi:10.1021/am4004733

Matos, J., Llano, B., Montaña, R., Poon, P. S., and Hidalgo, M. C. (2018). Design of Ag/and Pt/TiO_2-SiO_2 nanomaterials for the photocatalytic degradation of phenol under solar irradiation. *Environ. Sci. Pollut. Control Ser*. 25 (19), 18894–18913. doi:10.1007/s11356-018-2102-3

Mungondori, H. H., Tichagwa, L., and Green, E. (2015). Synthesis and glass immobilization of carbon and nitrogen doped TiO_2-SiO_2 and its effect on *E. coli* ATCC 25922 bacteria. *Br. J. Appl. Sci. Technol*. 5 (5), 447. doi:10.9734/bjast/2015/11049

Oriel-Instruments (1999). *The book of photon tools*. Stratford, CT: Oriel Instrument, 1–3.

Panayotov, D., and Yates, J. T. (2003). Bifunctional hydrogen bonding of 2-chloroethyl ethyl sulfide on TiO_2–SiO_2 powders. *J. Phys. Chem. B*. 107 (38), 10560–10564. doi:10.1021/jp0304273

Ramamoorthy, V., Kannan, K., Joseph, J., Infant, A., Kanagaraj, T., and Thiripuranthagan, S. (2016). Photocatalytic degradation of acid orange dye using silver impregnated TiO_2/SiO_2 composite catalysts. *J. Nanosci. Nanotechnol*. 16 (9), 9980–9986. doi:10.1166/jnn.2016.12071

Ren, Y., Chen, M., Zhang, Y., and Wu, L. (2010). Fabrication of rattle-type TiO_2/SiO_2 core/shell particles with both high photoactivity and UV-shielding property. *Langmuir* 26 (13), 11391–11396. doi:10.1021/la1008413

Shi, X., Lou, Z., Zhang, P., Fujitsuka, M., and Majima, T. (2016). 3D-Array of Au–TiO_2 yolk–shell as plasmonic photocatalyst boosting multi-scattering with enhanced hydrogen evolution. *ACS Appl. Mater. Interfaces* 8 (46), 31738–31745. doi:10.1021/acsami.6b12940

Singh, R., Bapat, R., Qin, L., Feng, H., and Polshettiwar, V. (2016). Atomic layer deposited (ALD) TiO_2 on fibrous nano-silica (KCC-1) for photocatalysis: nanoparticle formation and size quantization effect. *ACS Catal*. 6 (5), 2770–2784. doi:10.1021/acscatal.6b00418

Wang, T., Zhu, Y. C., Xu, Z. Y., Wu, L. G., Wei, Y. Y., Chen, T. N., et al. (2016). Fabrication of weak-room-light-driven TiO_2-based catalysts through adsorbed-layer nanoreactor synthesis: enhancing catalytic performance by regulating catalyst structure. *J. Phys. Chem. C*. 120 (22), 12293–12304. doi:10.1021/acs.jpcc.6b03721

Wei, Q., Li, Y., Zhang, T., Tao, X., Zhou, Y., and Chung, K., et al. (2014). TiO_2–SiO_2-composite-supported catalysts for residue fluid catalytic cracking diesel hydrotreating. *Energy Fuels* 28 (12), 7343–7351. doi:10.1021/ef500799t

Xu, Z., Huang, C., Wang, L., Pan, X., Qin, L., Guo, X., et al. (2015). Sulfate functionalized Fe_2O_3 nanoparticles on TiO_2 nanotube as efficient visible light-active photo-Fenton catalyst. *Ind. Eng. Chem. Res*. 54 (16), 4593–4602. doi:10.1021/acs.iecr.5b00335

Zangeneh, H., Zinatizadeh, A. A. L., Habibi, M., Akia, M., and Isa, M. H. (2015). Photocatalytic oxidation of organic dyes and pollutants in wastewater using different modified titanium dioxides: a comparative review. *J. Ind. Eng. Chem*. 26, 1–36. doi:10.1016/j.jiec.2014.10.043

Zhang, Y., Chen, J., Tang, H., Xiao, Y., Qiu, S., Li, S., et al. (2018). Hierarchically-structured SiO_2-Ag@ TiO_2 hollow spheres with excellent photocatalytic activity and recyclability. *J. Hazard Mater*. 354, 17–26. doi:10.1016/j.jhazmat.2018.04.047

Conflict of Interest: The authors declare that the research was conducted in the absence of any commercial or financial relationships that could be construed as a potential conflict of interest.